Scientia Iranica A (2014) 21(6), 1821–1832

SCIENTIA IRANICA

Sharif University of Technology

Scientia Iranica

Transactions A: Civil Engineering

www.scientiairanica.com

The influence of seepage and gravitational loads on elastoplastic solution of circular tunnels

A. Fahimifar[a,*], H. Ghadami[b] and M. Ahmadvand[b]

a. *Department of Civil and Environmental Engineering, Amirkabir University of Technology, Tehran, Iran.*
b. *Department of Civil Engineering, Tafresh University, Tafresh, Iran.*

Received 8 July 2013; received in revised form 7 February 2014; accepted 29 April 2014

KEYWORDS

Underwater tunnels;
Seepage;
Gravitational loads;
Elastoplastic solution;
Strain-softening.

Abstract. In this paper, an elastoplastic model is proposed to analyze the circular tunnels below a groundwater table under axial-symmetric conditions, considering the effects of seepage and gravitational loads. In the proposed method, the strain-softening behavior model and Hoek-Brown failure criterion are used. To evaluate the effect of gravitational loads and variations of pore pressure, the equations concerning different directions around the tunnel (crown, wall and floor) are derived. Since the derived differential equations do not have a closed-form solution in the plastic zone, the numerical finite difference method is applied. Considering the strain-softening behavior of the rock mass, the problem in the plastic zone is solved through a stepwise method, where the strength parameters of the rock mass vary, step-by-step, from their maximum values to the constant values. Besides, the stresses, strains, and deformations of the rock mass also vary step-by-step from the elastoplastic boundary to tunnel boundary values. Furthermore, the closed-form analytical solutions are obtained for the elastic zone. The accuracy and application of the proposed method are demonstrated by a number of examples. The results well exhibit the effects of dilatancy angle and increment of elastic strain in the plastic zone. Based on the results obtained, ignoring the effects of gravitational loads and seepage will definitely produce computational errors.

1. Introduction

The convergence-confinement method is the most commonly used method applied to tunnel design and analysis. Using this approach, the ground response curve is determined based on ground convergence to the internal pressure of the tunnel, and ground behavior is demonstrated based on this curve during the tunnel excavation. The proposed solutions for determination of ground response curves are divided into two groups, including closed-form analytical solutions and unclosed numerical-analytical solutions. Since, sometimes, a large number of simplifying assumptions are applied, the closed-form solutions are considered as approximate, while unclosed analytical-numerical approaches offer more accurate solutions, since they assess rock mass behavior through a more sophisticated approach. Through the convergence-confinement technique, the gravitational loads induced by the weight of the plastic zone in the crown and the floor of the tunnel are ignored. Indeed, due to the difference in gravitational loads in different directions around the tunnel, tunnel convergence enhances from its floor to its crown.

*. *Corresponding author. Tel.: +98 21 64543011;*
Fax: +98 21 64543011
E-mail addresses: Fahim@aut.ac.ir (A. Fahimifar); Hamed.ghadami@yahoo.com (H. Ghadami); m.ahmadvand@taha-ce.com (M. Ahmadvand)

When tunnel excavation is performed below the water table, tunnel behavior is greatly affected by seepage, which affects ground behavior and the ground response curve. Besides, in this state, the water flows into the tunnel and, as a result, seepage develops in the zones around it.

The stress and deformation fields formed by tunnel excavation and seepage in the tunnels below the water table have been investigated by many researchers. Although the majority of the proposed solutions are based on numerical approaches, few closed-form solutions proposed for tunnels can be found. Brown et al. [1], Alonso et al. [2], Park et al. [3], and Lee and Pietruszczak [4] proposed analytical solutions for elastoplastic analysis of a tunnel based on the strain-softening behavior of the rock mass. However, in these methods, the effects of gravitational loads and seepage have not been taken into account.

Brown and Bray [5], Lee et al. [6], and Shin et al. [7] considered the effects of seepage and pore pressure in their solutions. Also, Fahimifar and Zareifard [8] presented their analytical model by considering the seepage body forces and development of the exact Kolymbas and Wagner [9] seepage model. Fahimifar et al. [10] proposed a new elastoplastic solution for analysis of the tunnels below the water table by considering the strain-softening behavior of the rock mass. This model is based on mixing the exact seepage model of Ming et al. [11] (for the elastic zone) and the radial seepage model, by considering the hydraulic-mechanical coupling of the rock mass (for the plastic zone). In the model proposed by Fahimifar et al. [10], unlike other models, the effects of dilatancy angle variations and elastic strain increments in the plastic zone have also been taken into account. One of the few proposed solutions for tunnel analysis considering gravitational loads is that proposed by Zareifard and Fahimifar [12]. However, the effects of seepage and pore pressure have not been considered in their model.

In this research, an elastoplastic model is proposed for analysis of a tunnel below the groundwater table, considering the effects of seepage and gravitational loads, using the Hoek-Brown criterion and strain-softening behavior model. To evaluate the effect of gravitational and seepage loads, stress and pore pressure was calculated for different directions around the tunnel (crown, wall, and floor). Because of the variations of pore pressure and gravitational loads in different directions around the tunnel, and calculation of the stress, strain, and pore pressure at each point, the body forces induced by gravitational forces and pore pressure in the given point are applied in the corresponding equations of axisymmetric conditions. Therefore, simultaneous consideration of the effects of these two factors leads to deriving more accurate results compared to other proposed models.

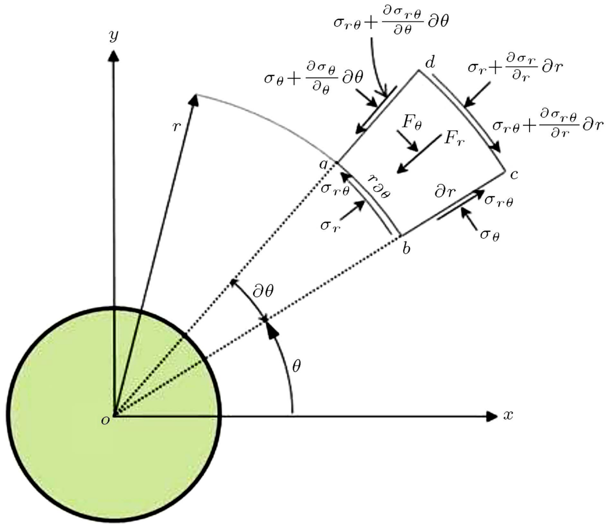

Figure 1. Body forces and stress components of a rock mass element.

2. Model assumptions and governing equations

The model involves different rock mass zones, including elastic and plastic zones (strain-softening and residual strength zones). Figure 1 presents all applied stresses and body forces on element "abcd" with unit thickness during excavation of a circular tunnel.

Based on Figure 1, the equilibrium expression in the radial direction can be derived as:

$$\frac{\partial\sigma_r}{\partial r}+\frac{1}{r}\frac{\partial\sigma_{r\theta}}{\partial\theta}-\frac{(\sigma_\theta-\sigma_r)}{r}+F_r=0, \tag{1}$$

where, σ_r is radial stress, σ_θ is circumferential stress, and F_r is the body force induced by the weight of fractured rock mass in a radial direction. Also, a similar equation can be obtained for the circumferential direction.

The gravitational load induced by the effect of fractured rock mass in the radial direction is expressed as Eq. (2) [12]:

$$F_r=\gamma\sin\theta, \tag{2}$$

where, γ is the specific weight of the rock mass, and F_r is the body force induced by the plastic zone of the rock mass in a radial direction. Considering Eq. (1), the equilibrium expression under the axial-symmetric condition in the plastic zone for elements of rock mass in the polar system is expressed as:

$$\frac{d\sigma_r}{dr}-\frac{(\sigma_\theta-\sigma_r)}{r}+F_r=0. \tag{3}$$

Under the axial-symmetric condition, deformation-strain equilibria will be as Eqs. (4) to (6) [13]:

$$\varepsilon_r = \frac{du}{dr}, \tag{4}$$

$$\varepsilon_\theta = \frac{u}{r}, \tag{5}$$

$$\frac{d\varepsilon_r}{dr} = \frac{\varepsilon_r - \varepsilon_\theta}{r}, \tag{6}$$

where, ε_r and ε_θ are radial and circumferential strains, respectively, while u is radial deformation.

3. Failure criterion of the rock mass and behavior model (stress-strain equation)

The failure criterion applied for the rock mass is the nonlinear empirical Hoek-Brown criterion, which is expressed as Eq. (7) [14]:

$$\sigma_\theta - \sigma_r = \left\{ m(\sigma_r - P_w)\sigma_c + s\sigma_c^2 \right\}^a, \tag{7}$$

where $\sigma_1 = \sigma_\theta$ and $\sigma_3 = \sigma_r$ are major and minor principal stresses in the failure point, respectively; P_w is pore pressure; σ_c is the uniaxial compressive strength of the rock mass; m and s are strength parameters of the rock mass; and a is the exponential coefficient of the Hoek Brown failure criterion. In this research, a is considered as 0.5.

In the present work, the strain-softening model of Alonso et al. [2] was applied as the behavior model. Rock mass will behave elastically until the failure criterion is satisfied. After that, the rock mass strength reaches gradually to the residual strength. Through the strain-softening model of Alonso et al. it is assumed that strength parameters, m and s, and dilatancy angle (ψ) is a bilinear function of deviatoric plastic strain (η) [2]:

$$w = \begin{cases} w_p - (w_p - w_r)\frac{\eta}{\eta^*} & 0 < \eta < \eta^* \\ w_r & \eta > \eta^* \end{cases} \tag{8}$$

where w represents one of the parameters m, s and ψ, and η^* is the critical deviatoric plastic strain from which the residual behavior starts, and should be identified by experiments. The subscripts 'p' and 'r' denote the peak and residual values, respectively.

It must be noted that, in this model, η is the strain-softening parameter for the control of parameters (s, m, σ_c, ψ), and is expressed as Eq. (9) [3]:

$$\eta = \varepsilon_\theta^p - \varepsilon_r^p. \tag{9}$$

In Eq. (9), ε_r^p and ε_θ^p are radial and circumferential plastic strains, respectively.

A comparison between the equations produced by two strain-softening models (i.e. Alonso et al. [2] and Brown et al. [1]) revealed that parameter η^* can be

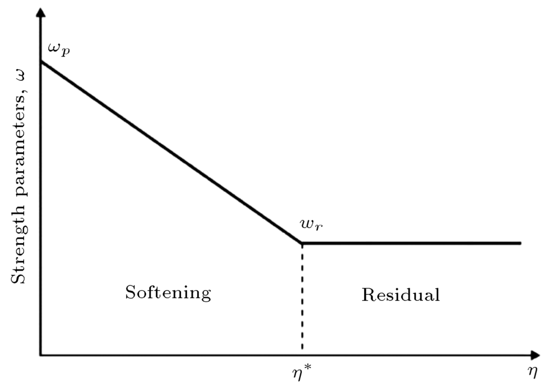

Figure 2. Variations of parameters s, m, σ_c and ψ in strain-softening model [4].

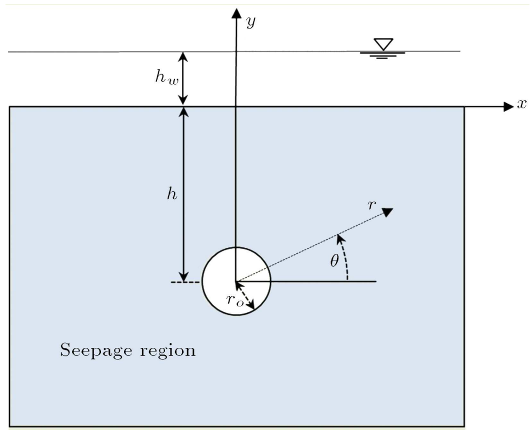

Figure 3. Geometry of the proposed seepage model.

estimated as [3]:

$$\eta^* = (\alpha - 1)\,\varepsilon_\theta(r_e), \tag{10}$$

where, $\varepsilon_\theta(r_e)$ is the circumferential strain in the elasto-plastic boundary and α is a parameter indicating the length of the strain-softening zone in the Brown et al. [1] method.

Figure 2 presents variations of parameters, s, m, σ_c and ψ, in the strain-softening model, with respect to η (deviatoric plastic strain) function.

4. Seepage and pore pressure pattern

Figure 3 exhibits a tunnel with an external radius of r_o at a depth of h below the ground surface. Water depth above the ground is h_w. To model pore pressure in all directions around the tunnel, the seepage pattern of Ming et al. [11] with polar coordinates was applied. Using the conformal mapping, Ming et al. [11] proposed an accurate seepage pattern for tunnels below the water table.

The pattern was presented based on the following assumptions:

- The circular tunnel is located in a completely saturated, homogenous, isotropic aquifer.

- The flow has reached the steady-state.
- The water table does not fluctuate with seepage.

In cases where the pore pressure is constant in the outer surface of the tunnel, the equation of Ming et al for calculation of pore pressure is presented as [11]:

$$P_w(x,y) = (h_w - y)\gamma + \frac{P_a + \gamma_w r \sin\left(\arctan\frac{h+y}{x}\right) - \gamma_w h - \gamma_w h_w}{2\ln\left[\frac{h}{r_o} - \sqrt{(\frac{h}{r_o})^2 - 1}\right]} \left(\ln\frac{x^2 + \left(y + \sqrt{h^2 - r_o^2}\right)^2}{x^2 + \left(y - \sqrt{h^2 - r_o^2}\right)^2}\right), \quad (11)$$

where r_o is the external radius of the tunnel; h is tunnel depth from the water table; h_w is water height above the ground surface; γ_w is the specific weight of water; and p_a is pore pressure in the outer surface of the tunnel.

Since the maximum water level is measured from the ground surface in the model presented in this work, h_w is taken as zero ($h_w = 0$). By replacing $x = r\cos\theta$ and $x = r\sin\theta - h$, pore water pressure in all directions of the tunnel can be calculated, based on the (r,θ) coordinate:

$$P_w(r,\theta) = (h - r\sin\theta)\gamma_w + \frac{P_a + \gamma_w r\sin\theta - \gamma_w h}{A} \left(\ln\frac{(r\cos\theta)^2 + \left(r\sin\theta - h + \sqrt{h^2 - r_o^2}\right)^2}{(r\cos\theta)^2 + \left(r\sin\theta - h - \sqrt{h^2 - r_o^2}\right)^2}\right), \quad (12)$$

where:

$$A = 2\ln\left(\frac{h}{r_o} - \sqrt{\left(\frac{h}{r_o}\right)^2 - 1}\right). \quad (13)$$

Also, hydraulic head distribution is derived using the Bernoulli equation ($H_w = y + P_w/\gamma_w = r\sin\theta - h + P_w/\gamma_w$) as:

$$H_w(r,\theta) = \frac{\frac{P_a}{\gamma_w} + r\sin\theta - h}{A} \left(\ln\frac{(r\cos\theta)^2 + \left(r\sin\theta - h + \sqrt{h^2 - r_o^2}\right)^2}{(r\cos\theta)^2 + \left(r\sin\theta - h - \sqrt{h^2 - r_o^2}\right)^2}\right). \quad (14)$$

5. Stresses and deformations in the rock mass

In the proposed model, the perimeter of the tunnel is divided into different zones (Figure 4):

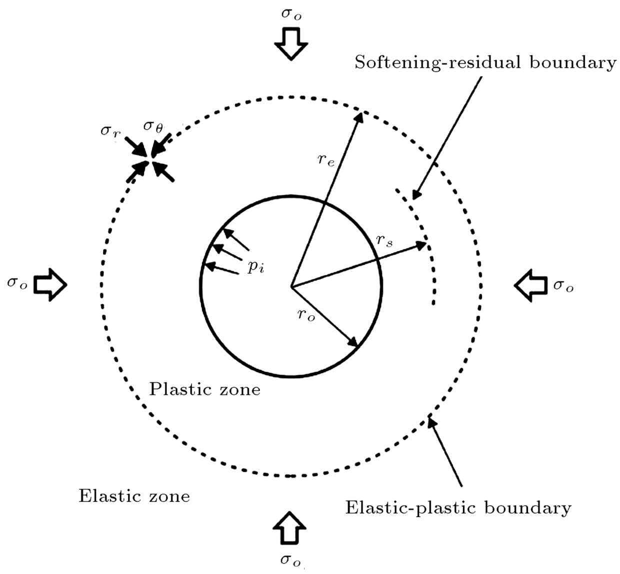

Figure 4. Circular tunnel in infinite plane [4].

- Elastic zone around the tunnel;
- Plastic zone between the elastic zone and the interior plastic zone where strain-softening behavior predominates;
- Interior plastic zone where the stress is limited to the residual strength.

5.1. Plastic zone

By replacing Eq. (7) (Hoek-Brown failure criterion) in Eq. (3), the equilibrium expression in the plastic zone is derived as:

$$\frac{d\sigma_r}{dr} + F_r = \frac{\left\{m(\sigma_r - P_w)\sigma_c + s\sigma_c^2\right\}^{\frac{1}{2}}}{r}. \quad (15)$$

To calculate the radial and circumferential strains in the plastic zone, the strain-displacement equation of the axisymmetric condition (Eq. (6)) is used. Unlike the Hoek-Brown model, which considers elastic strain as a constant throughout the plastic zone, the model proposed in this work calculates the increment of elastic strain in each ring, and it is considered separately. Thus, the total strain is divided into elastic and plastic strains:

$$\begin{Bmatrix}\varepsilon_r \\ \varepsilon_\theta\end{Bmatrix} = \begin{Bmatrix}\varepsilon_r^e \\ \varepsilon_\theta^e\end{Bmatrix} + \begin{Bmatrix}\varepsilon_r^p \\ \varepsilon_\theta^p\end{Bmatrix}. \quad (16)$$

The relationships between the elastic strain increments and the stress increments, $\Delta\sigma_r$ and $\Delta\sigma_\theta$, in the plastic zone are given by Hook's law [13]:

$$\begin{Bmatrix}\Delta\varepsilon_r^e(i) \\ \Delta\varepsilon_\theta^e(i)\end{Bmatrix} = \frac{1}{2G}\begin{bmatrix}1-v & -v \\ -v & 1-v\end{bmatrix}\begin{Bmatrix}\Delta\sigma_r(i) \\ \Delta\sigma_\theta(i)\end{Bmatrix}. \quad (17)$$

The Mohr-Coulomb criterion is used as the plastic potential function for a non-associated flow rule. For the Mohr-Coulomb type of plastic potential function, the relation between the plastic parts of the radial and circumferential strain increments is obtained as follows [15]:

$$\Delta\varepsilon_r^p = -K\Delta\varepsilon_\theta^p, \tag{18}$$

where, K is the dilation factor, and is given as [2]:

$$K = \frac{1+\sin\psi}{1-\sin\psi}. \tag{19}$$

In Eq. (19), ψ is the dilation angle and varies as a function of the softening parameter, η.

Since a multi-linear behavior model and the incremental theory of plasticity have been used, the governing equations on the stresses and strains in the plastic zone have no analytical solutions and must be solved numerically, as presented in Appendix A.

5.2. Elastic zone

Due to the fact that the body forces induced by the fractured zone weight do not affect the elastic zone, the equilibrium expression (Eq. (7)) in the elastic zone is defined as:

$$\frac{d\sigma_r}{dr} - \frac{(\sigma_\theta - \sigma_r)}{r} = 0. \tag{20}$$

Using the Hoek-Brown criterion, the stress-strain equation in the elastic zone under the axisymmetric plane stress condition is expressed as [8]:

$$\sigma_r = \frac{E_r}{(1+v_r)(1-2v_r)}\left[(1-v_r)\varepsilon_r + v_r\varepsilon_\theta\right], \tag{21}$$

$$\sigma_\theta = \frac{E_r}{(1+v_r)(1-2v_r)}\left[(1-v_r)\varepsilon_\theta + v_r\varepsilon_r\right]. \tag{22}$$

Substituting Eqs. (21) and (22) into Eq. (20), Eq. (23) for the deformation in the elastic zone is obtained:

$$\frac{d^2u_r}{dr^2} + \frac{1}{r}\frac{du}{dr} - \frac{u_r}{r^2} = 0. \tag{23}$$

Taking into account the appropriate boundary conditions, stresses, strains and deformations in the elastic zone are derived by solving the differential equation (Eq. (23)) (see details in Appendix B).

6. Validation of the proposed model

To validate the proposed model, a program was designed using the MATLAB code. Using this program, a few illustrative examples were analyzed and the results obtained were compared with those obtained from other models.

6.1. Example 1

In this example, the proposed model is compared with those proposed by Lee and Pietruszczak [4] and Park et al. [3] by ignoring the effects of seepage and gravitational loads. Data for the tunnel analyzed in Lee's model are introduced in Table 1.

The data obtained from tunnel analysis using the proposed method compared to those produced by Park's and Lee's methods for 5000 rings ($n = 5000$) are shown in Figure 5. As illustrated in the figure, in the case where the number of rings is selected large enough, the results obtained from the proposed method fit well with those produced by Lee's and Park's methods for different dilatancy (ψ) angles.

Figure 6 compares the ground deformation in terms of radial distance using the proposed method and

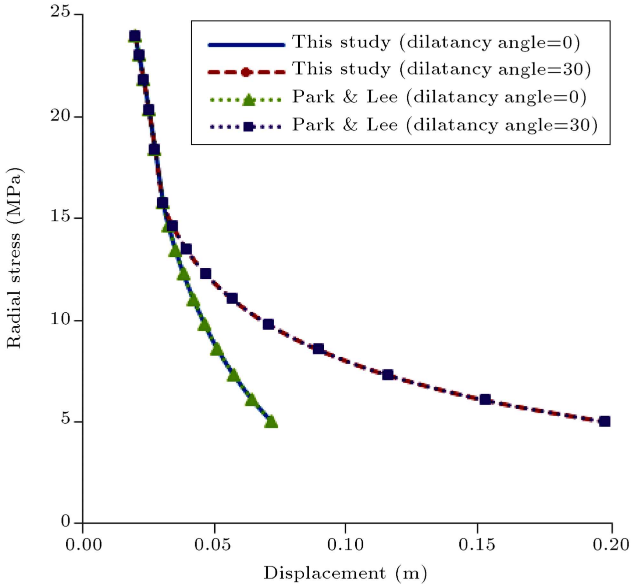

Figure 5. A comparison between ground response curves using the proposed method with ground response curve developed by Lee's [4] and Park's [3] methods in dry condition.

Table 1. Data derived from Lee's model [4].

Parameter	Value	Parameter	Value	Parameter	Value
E	5500	m_p	1.7	σ_o	30 MPa
v	0.25	s_p	0.0039	P_i	5 MPa
σ_c	30 MPa	m_r	1.0	A	0.5
ϕ_p	30	s_r	0	η^*	0.004742
r_o	5 m				

Table 2. Data of the method proposed by Brown and Bray [5] for $h = 300$ m.

Parameter	Value	Parameter	Value	Parameter	Value
E	20000 MPa	m_p	0.65	p_o	27 MPa
v	02	m_r	0.2	P_i	1.98 MPa
σ_c	40 MPa	s_p	0.2	r_o	3.0 m
ϕ_p	30	s_r	0.0001	h	300 m
A	0.5				

Table 3. A comparison between the results obtained from the method of Brown and Bray [5] and the proposed method for $h = 300$ m.

Parameter	Brown and Bray method [5]	Tunnel program		
		$\psi = 0$	$\psi = \phi/4$	$\psi = \phi/2$
Elasto-plastic radius (re) (m)	16.024	20.044	20.404	20.758
Radial stress at elastoplastic radius (σ_{re}) (MPa)	16.73	16.833	16.836	16.838
Tunnel convergence (m)	0.1434	0.1281	0.222	0.4661

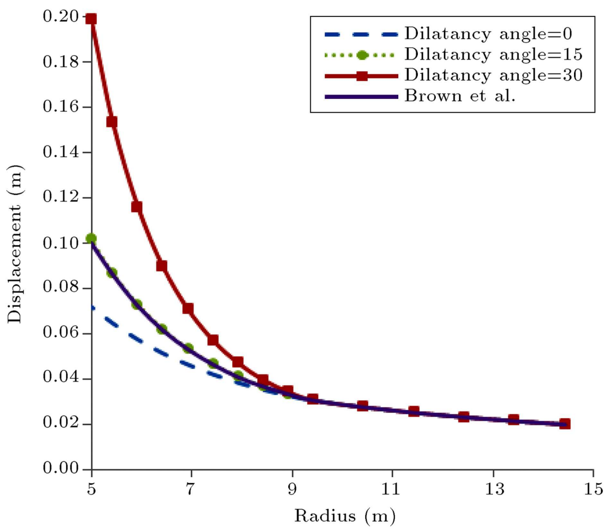

Figure 6. Ground deformation in terms of radial distance for different dilatancy (ψ) angles in dry condition.

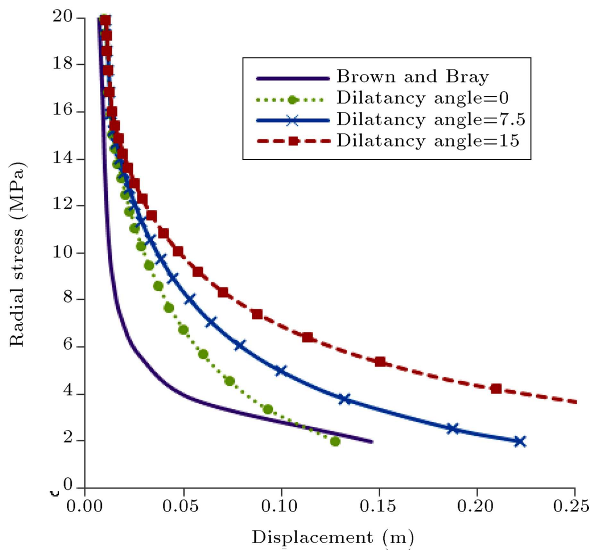

Figure 7. Ground response curve obtained from the proposed method and the method of Brown and Bray [5] for $h = 300$ m.

the method proposed by Brown et al. [1] for different dilatancy (ψ) angles. As shown in the figure, ground deformation in this method is similar to the ground deformation obtained by the proposed method for a dilatancy angle of 15°. As ψ increases from 0 to 30°, ground deformation in the tunnel walls rises from 0.072 for $\psi = 0°$ to 0.0196 for $\psi = 30°$.

6.2. Example 2

A tunnel was excavated in rock with limestone and siltstone at a depth of 300 m below the groundwater table (Table 2). Considering the properties of this tunnel, Brown and Bray analyzed the tunnel and published the results obtained in their paper. They ignored the effects of gravitational loads and pore pressure variations in their model and generalized the results of the horizontal direction (tunnel wall) for all directions of the tunnel.

The results obtained from the Brown and Bray [5] model and the proposed method are compared in Table 3. As the table shows, by increasing values of ψ, the elastoplastic radius and ground deformation rise prior to lining installation. Moreover, due to taking into account the elastic strain increment in the plastic zone of the model proposed in the present study, greater values are obtained for the elastoplastic radius compared to the method proposed by Brown and Bray [5]. Furthermore, the radial and circumferential stresses in the elastoplastic boundary highly correspond with those of the Brown and Bray [5] method, because of the analytical similarity between the elastic zone of the proposed method and the method of Brown and Bray.

Figure 7 illustrates ground response curves pro-

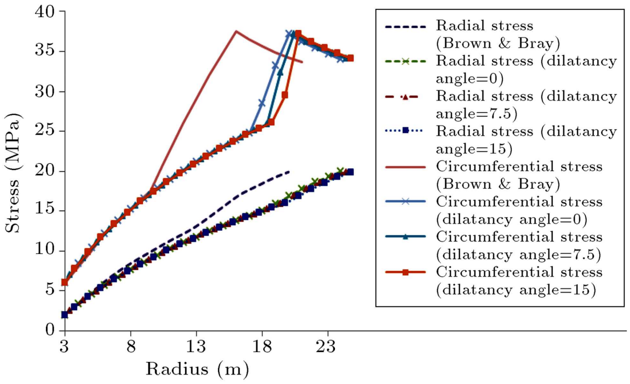

Figure 8. A comparison between circumferential and radial stresses in the tunnel wall in terms of the radial distance derived from the proposed method and the model of Brown and Bray [5] ($h = 300$ m).

duced by the method of Brown and Bray [5] and the proposed method for the tunnel wall. As ψ rises from to 0° to 15°, the ground response curve considerably changes; by increasing the ψ tunnel convergence prior to the lining installation increases from 0.128 for $\psi = 0°$ to 0.466 for $\psi = 15°$.

Also, Figure 8 exhibits radial and circumferential stresses (σ_r and σ_θ) for the tunnel wall in terms of radius (r) calculated by the method of Brown and Bray [5] and the proposed method for different dilatancy angles. Likewise, in the model proposed by Brown and Bray [5], stress-strain analysis was performed by taking into account the strain-softening behavior and Hoek-Brown failure criterion; however, the effect of dilatancy angle variations and increments of elastic strain in the plastic zone were not considered. Moreover, in the method of Brown and Bray [5] the radial seepage model was applied. In contrast, in the proposed method, not only was the hydraulic analysis performed by the more accurate non-radial seepage model of Ming et al. [11], but the elastic strain in the plastic zone was measured based on dilatancy angle. Also, the effect of ψ on tunnel performance in the plastic zone is considered.

Considering the effect of ψ and elastic strain increment in the plastic zone, the elastoplastic radius increases by increasing dilatancy angle. Moreover, by maintaining the lining pressure in the proposed model, ground deformation increases significantly by increasing dilatancy angle.

Figure 9 illustrates pore pressure in three directions, including vertical to the tunnel crown (a), horizontal (b), and perpendicular to the tunnel floor (c) using the Ming et al. [11] seepage model. As shown in the figure, the results obtained from the Ming model well fit with those produced by the FLAC program and have high accuracy for modeling the pore pressure in all directions around the tunnel.

In Figures 10 and 11, ground response curves and

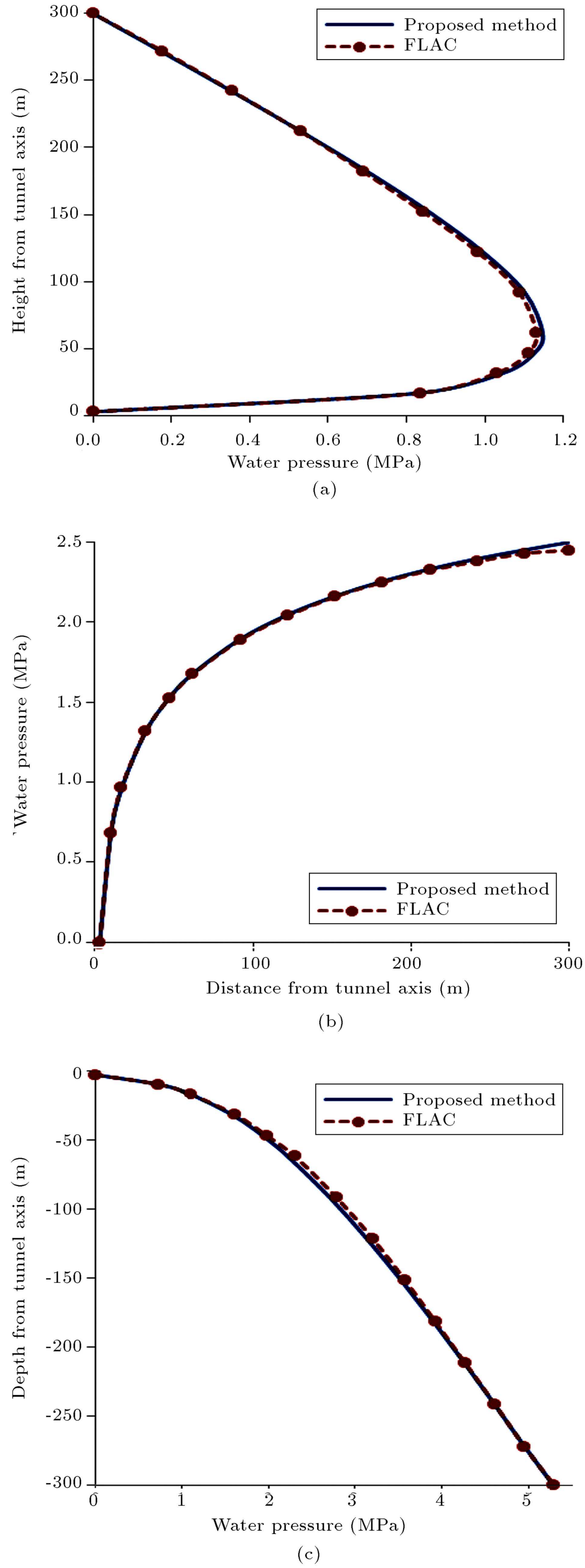

Figure 9. Pore pressure distribution in different directions around the tunnel: a) Vertical to the tunnel crown; b) horizontal direction; and c) perpendicular to the tunnel floor.

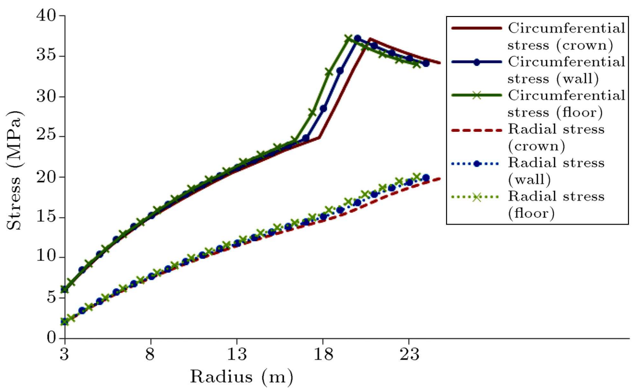

Figure 10. Radial and circumferential stress variations for wall, floor, and crown of the tunnel.

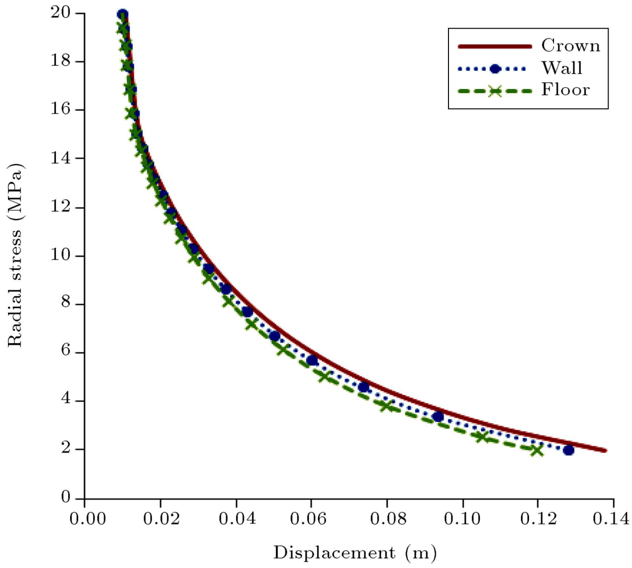

Figure 11. Ground response curves for wall, crown, and floor of the tunnel.

variations of radial and circumferential stresses on the wall, crown and floor of the tunnel are presented by taking into account the effects of gravitational and seepage loads (dilatancy angle is constant). Ground displacement and the elastoplastic radius of the tunnel increase from the floor to the crown of the tunnel, as it increases from 0.12 m in the tunnel floor to 0.1375 m in the tunnel crown. In addition, elastoplastic radius rises from 19.49 m in the tunnel floor to 20.75 m in the tunnel crown. Thus, the gravitational loads act as an instability factor in the crown and as a stability factor in the floor.

Figures 12 and 13 illustrate that the ground response curves of the crown and floor of the tunnel are compared for three cases, including:

1. Dry condition;
2. Taking into account the effect of seepage (but not gravitational load);

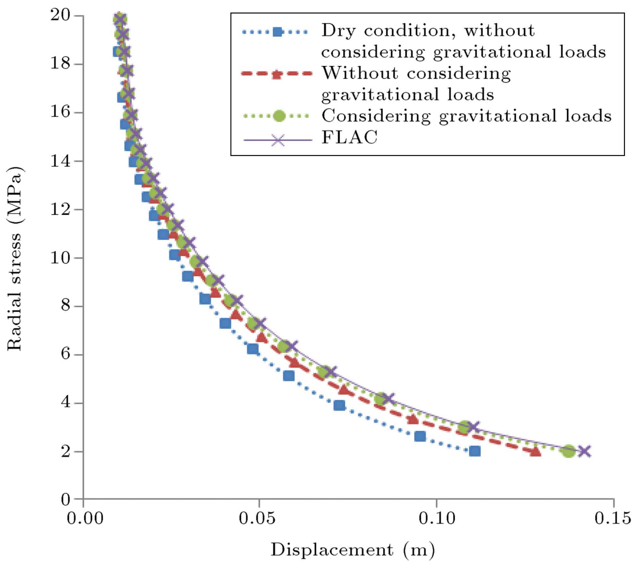

Figure 12. Ground response curve in the tunnel crown.

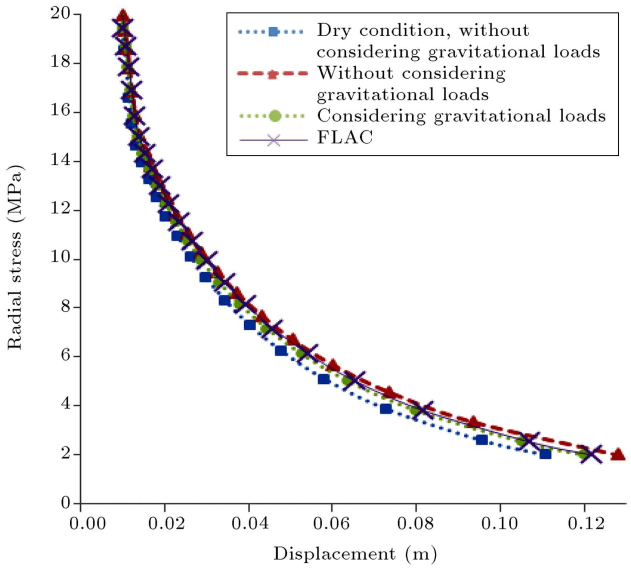

Figure 13. Ground response curve in the tunnel floor.

3. Taking into account both the effects of seepage and gravitational loads with the results of the FLAC program.

According to Figure 12, considering the effect of seepage and gravitational loads, ground deformation increases compared to the case of dry conditions in the tunnel crown. In other words, both seepage and gravitational load factors negatively affect tunnel stability.

Ground deformation in the tunnel floor increases in the case of taking the effect of seepage into account compared to dry conditions; but it drops in the tunnel bottom in the case of applying gravitational loads. It means that the gravitational loads positively affect stability in the floor of the tunnel (Figure 13).

7. Conclusion

In this research, a novel stepwise method using the numerical FDM was proposed for the elastoplastic analysis of underwater tunnels, taking into account the effects of seepage and gravitational loads. The accuracy and performance of the proposed model were compared with the model proposed for the elastoplastic analysis of a tunnel by Park et al. [3], and the method proposed for tunnel analysis below the water table proposed by Brown and Bray [5]. In the proposed model, in each step, 1 mm is added to the diameter length; for Examples 1 and 2, 3000 and 5000 rings are required, respectively, for satisfying the boundary conditions in each calculation of the elastoplastic radius. Considering the number of applied rings, the computations are performed with high accuracy for each radius of rock mass around the tunnel. The results derived from this work are summarized as:

- Unlike the model proposed by Brown and Bray [5], elastic and plastic strain increments are separately calculated for each ring in this research. Therefore, the elastoplastic radius rises compared to that of the Brown and Bray [5] method. By increasing dilatancy angle (ψ), plastic strain increases in each ring, which, in turn, leads to an increase in rock mass deformation and elastoplastic radius.
- Considering the fact that applying the radial seepage model for shallow tunnels is not accurate, because of considerable errors, the exact non-radial Ming et al. [11] model was applied in the present study to model pore pressure distribution around the tunnel. Using this model allows calculating the pore pressure at each point around the tunnel. Based on the results obtained, elastoplastic radius and tunnel convergence rises as the seepage effect is taken into account.
- Regarding the ground response curve for the crown and floor of the tunnel, it is required to calculate plastic zone weight and variations of pore pressure in the tunnel. Due to the significant effect of gravitational loads and seepage on tunnel stability in the crown and floor of the tunnel, ignoring the plastic zone weight may induce considerable errors.

Nomenclature

r	Radial distance from the center of the tunnel
θ	Angle measured clockwise from horizontal direction
σ_r	Radial stress
σ_θ	Circumferential stress
σ_1	Major principal stress
σ_3	Minor principal stress
ε_r	Radial strain
ε_θ	Circumferential strain
ε_1	Major principal strain
ε_3	Minor principal strain
w	Expresses parameters m, s, σ_c, ψ
w_p	Parameters m, s, σ_c, ψ for intact rock mass
w_r	Parameters m, s, σ_c, ψ for broken rock mass
$\bar{w}$	Parameters m, s, σ_c, ψ for different elements
m, s	Material constants of Hoek-Brown failure criterion
ψ	Dilatancy angle
σ_c	Uniaxial compressive strength of intact rock
E	Deformability modulus of rock mass
v	Poisson's ratio of rock mass
ϕ_p	Friction angle
a	Exponential coefficient of Hoek-Brown criterion
r_o	Radius of tunnel
r_e	Elastoplastic radius
r_s	External radius of residual zone
h	Depth of the tunnel from ground surface
h_w	Water depth above the ground surface
H_w	Water head
P_w	Pore water pressure in the rock mass
P_a	Water pressure on the perimeter of the tunnel
σ_o	Initial stress
P_i	Tunnel internal pressure
γ_w	Specific weight of water
γ	Specific weight of the rock mass
η^*	Parameter indicating the length of strain-softening zone in Alonso's method
η	Strain-softening function
α	Parameter indicating the length of strain-softening zone in Brown's method
F_r	Body forces in radial direction
F_θ	Body forces in circumferential direction

Superscripts

p	Refers to quantities corresponding to plastic zone

e Refers to quantities corresponding to elastic zone

References

1. Brown, E.T., Bray, J.W., Ladanyi, B. and Hoek, E. "Ground response curves for rock tunnels", *J. Geotech. Eng.*, **109**(1), pp. 15-39 (1983).

2. Alonso, E., Alejano, L.R., Varas, F., Fdez-Manin, G. and Carranza-Torres, C. "Ground response curves for rock masses exhibiting strain-softening behavior", *Int. J. Numer. Anal. Meth. Geomech.*, **27**(13), pp. 1153-1185 (2003).

3. Park, K.-H., Tontavanich, B. and Lee, J.-G. "A simple procedure for ground response curve of circular tunnel in elastic-strain softening rock masses", *Tunn. Undergr. Space. Technol.*, **23**(2), pp. 151-159 (2008).

4. Lee, Y.-K. and Pietruszczak, S. "A new numerical procedure for elasto-plastic analysis of a circular opening excavated in a strain-softening rock mass", *Tunn. Undergr. Space. Technol.*, **23**(5), pp. 588-599 (2008).

5. Brown, E. and Bray, J. "Rock-support interaction calculations for pressure shafts and tunnels", *ISRM Sym., Rock Mechanics Related to Caverns and Pressure Shafts*, Aachen, Germany, A.A. Balkema, pp. 26-28 (1982).

6. Lee, S., Jung, J., Nam, S. and Lee, I. "The influence of seepage forces on ground reaction curve of circular opening", *Tunn. Undergr. Space. Technol.*, **22**(1), pp. 28-38 (2006).

7. Shin, Y.J., Kim, B.M., Shin, J.H. and Lee, I.M. "The round reaction curve of underwater tunnels considering seepage forces", *Tunn. Undergr. Space. Technol.*, **25**(4), pp. 315-324 (2010).

8. Fahimifar, A. and Zareifard, M.R. "A thoretical solution for analysis of tunnels below groundwater considering the hydraulic-mechanical coupling", *Tunn. Undergr. Space. Technol.*, **24**(6), pp. 634-646 (2009).

9. Kolymbas, D. and Wagner, P. "Groundwater ingress to tunnels - the exact analytical solution", *Tunn. Undergr. Space. Technol.*, **22**(1), pp. 23-27 (2007).

10. Fahimifar, A., Ghadami, H., Ahmadvand, M. and Abdolmaleki, A. "Analysis of underwater tunnels considering strain-softening brhavior in plastic zone", *Tunn. Undergr. Space. Eng.*, **1**(1), pp. 13-28 (2013) (in Persian).

11. Ming, H., Meng-Shu, W., Tan, Z.-S. and Xiu-Ying, W. "Analytical solution for steady seepage into an underwater circular tunnel", *Tunn. Undergr. Space. Technol.*, **25**(4), pp. 391-396 (2010).

12. Zareifard, M.R. and Fahimifar, A. "A new solution for shallow and deep tunnels by considering the gravitational loads", *Acta. Geotech. Slov.*, **2012**(2) (2012).

13. Timoshenko, S. and Goodier, J., *Theory of Elasticity, McGraw-Hill*, New York (1994).

14. Hoek, E. and Brown, E. "Empirical strength criterion for rock masses", *J. Geotech. Eng., Asce*, **106**(GT9), pp. 1013-1035 (1980).

15. Ghadami, H., *Stability Analysis of Pressure Tunnels by Considering Seepage Effect*, MSc Dissertation, Dept of Civil Eng., Tafresh Univeristy, Tafresh, Iran (2012).

Appendix A: Stress-strain analysis in plastic zone

According to Section 5.1 (Eq. (15)), equilibrium expression in the plastic zone is derived as:

$$\frac{d\sigma_r}{dr}+F_r=\frac{\left\{m(\sigma_r-P_w)\sigma_c+s\sigma_c^2\right\}^{\frac{1}{2}}}{r}. \tag{A.1}$$

Since introducing a closed-form solution is impossible for solving the above differential equation, the equations are solved using the numerical solution of the Finite Difference Method (FDM).

Using the numerical FDM solution of Eq. (15), radial stress in each ring can be solved as:

$$\sigma_r(i)=\sigma_r(i-1)-F_r\Delta r(i)+B(i)+\sqrt{B^2(i)+2B(i)\left(\sigma_r(i-1)-\overline{P_w}(i)\right)+C(i)}, \tag{A.2}$$

where:

$$\lambda(i)=\frac{r(i)-r(i-1)}{r(i)+r(i-1)},$$

$$C(i)=\bar{s}(i).\overline{\sigma_c}^2(i),$$

$$B(i)=\frac{\bar{m}(i)\overline{\sigma_c}^2(i)}{\lambda(i)},$$

$$\Delta r(i)=r(i)-r(i-1),$$

$$\overline{P_w}(i)=\frac{1}{2}\left(P_w(i-1)+P_w(i)\right),$$

$$\bar{m}(i)=\frac{1}{2}\left(m(i-1)+m(i)\right),$$

$$\bar{s}(i)=\frac{1}{2}\left(s(i-1)+s(i)\right),$$

$$\overline{\sigma_c}(i)=\frac{1}{2}\left(\sigma_c(i-1)+\sigma_c(i)\right). \tag{A.3}$$

Parameters $s(i)$, $m(i)$ and $\sigma_c(i)$ are expressed in terms of η (deviatoric plastic strain). Using the numerical FDM solution of Eq. (9), Eq. (A.4) is obtained for each ring:

$$\eta(i)=\eta(i-1)+\left(\Delta\varepsilon_\theta^p(i)-\Delta\varepsilon_r^p(i)\right). \tag{A.4}$$

The total strain is divided into elastic and plastic strains:

$$\begin{Bmatrix} \varepsilon_r \\ \varepsilon_\theta \end{Bmatrix} = \begin{Bmatrix} \varepsilon_r^e \\ \varepsilon_\theta^e \end{Bmatrix} + \begin{Bmatrix} \varepsilon_r^p \\ \varepsilon_\theta^p \end{Bmatrix}. \tag{A.5}$$

By replacing Eq. (16) in Eq. (6) and solving the resultant equation by FDM, $\Delta\varepsilon_\theta^P(i)$ (increment of circumferential plastic strain), is obtained by:

$$\Delta\varepsilon_\theta^p(i) = P_1/P_2,$$

$$P_1 = -\Delta\varepsilon_\theta^e(i) + \lambda(i)\left[\frac{1+\nu}{E}\left(\Delta\sigma_r(i) - \Delta\sigma_\theta(i)\right)\right.$$

$$\left. + 2\left(\varepsilon_r(i-1) - \varepsilon_\theta(i-1)\right)\right],$$

$$P_2 = 1 + \lambda(i)\left(K(i) + 1\right), \tag{A.6}$$

where:

$$K(i) = \frac{1+\sin\varphi}{1-\sin\varphi}, \tag{A.7}$$

$$\lambda(i) = \left[\frac{r(i) - r(i-1)}{r(i) + r(i-1)}\right]. \tag{A.8}$$

In Eq. (A.6), $\varepsilon_\theta(i-1)$ and $\varepsilon_r(i-1)$ are circumferential and radial strains calculated, respectively, in the previous ring $(i-1)$. Here, $\Delta\varepsilon_\theta^e(i)$ and $\Delta\varepsilon_r^e(i)$ (circumferential and radial elastic strain increments) also are obtained from Eq. (A.9) [13]:

$$\begin{Bmatrix} \Delta\varepsilon_r^e(i) \\ \Delta\varepsilon_\theta^e(i) \end{Bmatrix} = \frac{1}{2G}\begin{bmatrix} 1-v & -v \\ -v & 1-v \end{bmatrix}\begin{Bmatrix} \Delta\sigma_r(i) \\ \Delta\sigma_\theta(i) \end{Bmatrix},$$

$$\begin{Bmatrix} \Delta\sigma_r(i) \\ \Delta\sigma_\theta(i) \end{Bmatrix} = \begin{Bmatrix} \sigma_r(i) - \sigma_r(i-1) \\ \sigma_\theta(i) - \sigma_\theta(i-1) \end{Bmatrix}. \tag{A.9}$$

After calculating $\Delta\varepsilon_\theta^p(i)$ from Eq. (A.6), $\Delta\varepsilon_r^p(i)$ can be obtained from Eq. (A.10) [3]:

$$\Delta\varepsilon_r^p(i) = -K(i)\Delta\varepsilon_\theta^p(i). \tag{A.10}$$

In this step, the plastic strain also can be calculated using the parameters measured in the previous steps:

$$\begin{cases} \varepsilon_r^p(i) = \varepsilon_r^p(i-1) + \Delta\varepsilon_r^p(i) \\ \varepsilon_\theta^p(i) = \varepsilon_\theta^p(i-1) + \Delta\varepsilon_\theta^p(i) \end{cases} \tag{A.11}$$

And the total circumferential and radial stresses are expressed from the total elastic and plastic strains:

$$\begin{Bmatrix} \varepsilon(i) \\ \varepsilon_\theta(i) \end{Bmatrix} = \begin{Bmatrix} \varepsilon_r(i-1) \\ \varepsilon_\theta(i-1) \end{Bmatrix} + \begin{Bmatrix} \Delta\varepsilon_r^e(i) \\ \Delta\varepsilon_\theta^e(i) \end{Bmatrix} + \begin{Bmatrix} \Delta\varepsilon_r^p(i) \\ \Delta\varepsilon_\theta^p(i) \end{Bmatrix}. \tag{A.12}$$

Finally, after computing the total circumferential strains, displacement can be calculate by Eq. (A.13):

$$u(i) = \varepsilon_\theta(i)r(i). \tag{A.13}$$

To solve this equation, first, an elastoplastic radius (r_e) is taken into account and then the calculations are performed in the elastoplastic boundary using the elastic zone equations. Next, considering the obtained stress and strain values in the elastoplastic boundary as initial values, Eqs. (A.2) to (A.13) are numerically solved until satisfying boundary conditions. The calculations are continued until the elastoplastic radius limits to a constant value [15].

Appendix B: Stress-strain analysis in elastic zone

According to Section 5.2 (Eq. (23)), the displacement expression in the elastic zone is derived as:

$$\frac{d^2u_r}{dr^2} + \frac{1}{r}\frac{du}{dr} - \frac{u_r}{r^2} = 0. \tag{B.1}$$

Eq. (B.1) can be solved analytically by applying the boundary conditions:

$$\begin{cases} \sigma_r|r \to \infty = \sigma_o \\ \sigma_r|r = r_e = \sigma_r(r_e) \end{cases} \tag{B.2}$$

Stress, strain, and deformation in the elastic zone are calculated using Eqs. (B.3) through (B.7):

$$u_r = \frac{1+\nu_r}{E_r}\left[\left[\sigma_o - \sigma_r(r_e)\right]\left(\frac{r_e^2}{r}\right) + \sigma_o(1-2v_r)r\right], \tag{B.3}$$

$$\varepsilon_\theta = \frac{1+\nu_r}{E_r}\left[\left[\sigma_o - \sigma_r(r_e)\right]\left(\frac{r_e^2}{r^2}\right) + \sigma_o(1-2v_r)\right], \tag{B.4}$$

$$\varepsilon_r = \frac{1+\nu_r}{E_r}\left[-\left[\sigma_o - \sigma_r(r_e)\right]\left(\frac{r_e^2}{r^2}\right) + \sigma_o(1-2v_r)\right], \tag{B.5}$$

$$\sigma_r = -\left[\left(\sigma_o - \sigma_r(r_e)\right)\left(\frac{r_e}{r}\right)^2\right] + \sigma_o, \tag{B.6}$$

$$\sigma_\theta = \left[\left(\sigma_o - \sigma_r(r_e)\right)\left(\frac{r_e^2}{r}\right)\right] + \sigma_o. \tag{B.7}$$

In Eqs. (B.3) to (B.7), the portion $\sigma_o(1-2v)$ that belongs to the initial displacements and strains of the ground, must be decreased from the final displacements and strains [8].

By replacing the radial and circumferential stresses in the elastoplastic boundary in the Hoek-Brown failure criterion and solving the equation obtained, the radial stress in the elastoplastic boundary is calculated using Eq. (B.8):

$$\sigma_r(r_e) = \sigma_o + \frac{1}{2}[D_1 - (D_1^2 + 4D_1(\sigma_o - P_w(r_e)) + s\sigma_c^2)^{\frac{1}{2}}], \tag{B.8}$$

where:

$$D_1 = \frac{m\sigma_c}{4}. \tag{B.9}$$

Biographies

Ahmad Fahimifar obtained a BS degree in Civil engineering at Iran University of Science and Technology, Tehran, Iran, in 1976. After a period in industry, he obtained an MS degree from the University of Birmingham, UK, and a PhD degree from the University of Newcastle Upon Tyne, UK, in 1990, for his work on the behavior of jointed rocks.

He is currently Professor and Head of the Civil Engineering Department at Amirkabir University of Technology, and has delivered many lectures on rock mechanics and tunnel engineering. He is a member of the International Society for Rock Mechanics, founder and member of the Iranian Society for Rock Mechanics, the Iran Tunneling Association, and the Iranian Society of Civil Engineers. He is also member of the editorial board of some research journals, including: Tunnelling and Underground Space Engineering, Amirkabir Journal of Science and Technology, and the Journal of Engineering Geology and the Environment.

Hamed Ghadami obtained his BS degree in Mechanical Engineering (fluid mechanics) from Iran University of Science and Technology, Tehran, Iran, in 2009, and his MS degree in Civil Engineering (geotechnical engineering) from Tafresh University, Iran, in 2012. Currently he is geotechnical expert in the Alborz Regional Water Company, in Karaj, Iran. His main topics of research are analytical and numerical methods in geomechanics, underwater tunnels, pressure tunnels, foundation engineering, slope stability, seepage and pore pressure distribution, and he is author of several papers on subjects related to rock mechanics, geotechnical engineering, tunnel engineering and numerical modeling.

Masoud Ahmadvand obtained his BS degree in Solid Mechanics Engineering from Tabriz University, Iran, in 2008, and his MS degree in Soil Mechanics and Foundation Engineering from Tafresh University, Iran, in 2011. His research interests include finite element modeling of soil and rock-structures such as soil and concrete dam, slope and tunnel, assessment and control of geotechnical risks in geotechnical structures, analytical methods in geomechanics, and he has published several papers in the fields of rock foundations, rock slope and liquefaction and seepage in tunnels in different journals and at international conferences. He also contributes in Taha Consulting Engineers Co. in projects including geotechnical studies of soil dams, tunnels and ditches.